IEEE Access
Multidisciplinary | Rapid Review | Open Access Journal

SPECIAL SECTION ON DATA-DRIVEN MONITORING, FAULT DIAGNOSIS AND CONTROL OF CYBER-PHYSICAL SYSTEMS

Received January 26, 2018, accepted February 27, 2018, date of publication March 8, 2018, date of current version March 19, 2018.

Digital Object Identifier 10.1109/ACCESS.2018.2813667

Development and Performance Test of a Height-Adaptive Pesticide Spraying System

TINGKAI CHEN AND FEI MENG, (Member, IEEE)
Merchant Marine College, Shanghai Maritime University, Shanghai 201306, China

Corresponding author: Fei Meng (feimeng@shmtu.edu.cn)

This work was supported by the Shanghai Association for Science and Technology under Grant 16391902702.

ABSTRACT This paper investigate an adaptive pesticide spraying system according to the plants height. The system including a depth sensor and a spraying system with multiple nozzles at different height in vertical direction. The entire system is installed on an automatic guided vehicle. In order to implement precision spraying or automatic targeting, plant identification, and plant height calculation are critical for the system with fixed height of nozzles. The designed system will open one or combination of the nozzles of the spraying system since the plant height is identified. To address the plant height-adaptive challenge, a pesticide spraying system with plant height-adaptive is proposed based on a camera sensor to dealt with the figure of the plant. Both of the depth and color data of the figure are obtained and analyzed, the open or close state of the spraying system is optimized for different plants with different height. Various experimental results have demonstrated that the proposed system is considered as well.

INDEX TERMS Automatic guided vehicle, precision spraying, depth sensor, height-adaptive, signal processing.

I. INTRODUCTION

During past decade, these issue of environment pollution, reduction of production costs and concerns for healthfulness of food have been growing. These problems are caused by pesticide abuse in agriculture aspect. So the reduction of pesticide using plays a vital role [1]–[3]. To avoid above problems caused by using pesticides, the methods can be included: selection of resistant varieties, improve management techniques, application of organisms [4], [5]. However, selective spraying is main method to reduce pesticide using for growing plant. Selective spraying can be enabled only when and where it is needed instead of spraying whole fields evenly [6]–[8]. On the other hand, with the development of both agricultural mechanization and robot intelligence, automatic guided vehicle (AGV) with selective spraying system has been extensively applied to agriculture development for controlling pests and diseases [9]–[11]. Commonly, this kind of system will include plant detection part, system controllers and spray section with multiple nozzles in different height. These nozzles should be turned on or off independently according to sensor data. Therefore, extraction information of plant is precondition of precision spray. In this paper, plant information is obtained by Kinect® sensor through image processing.

Although there has been some work on pesticide precision spraying for plants on the basis of obtaining plant information [12]–[14]. At present, the sensors used for pesticide precision spraying system mainly include laser, infrared and ultrasound and vision [15]. In [16]–[18], ultrasonic sensor is used to measure tree width, and proportional solenoid valves are used to control sprayer flow rate to realize precision spray. The method is validated by metal tracer, and the results show that pesticide deposits is lower than conventional methods. In addition, according to many researchers, such as both [15], [19], the authors measure volume of canopy automatically with LIDAR and ultrasonic. The results show that both ultrasonic and LIDAR have a good correlation with manual method in aspect of volume estimation. Furthermore, in [20], Lin *et al.* use silhouetted plant image to extract plant information, for example, plant height and leaf area. All the experiments are carried out without destroying the plant itself. Besides, the Doruchowski and Holownicki [3] describe two system: shielded system and detection system. In gap area among trees, all nozzles are closed, in other words, its aims to apply pesticide only when and where needed by using ultrasonic and optical sensors. In addition to the above methods of detection information for plants. In [21] and [22], Sui and Thomasson and Fricke and Wachendorf developed a

ground-based sensing system with ultrasonic sensor to determine cotton plant height. The wetland vegetation height is estimated in [23], Luo *et al.*use air borne LiDAR data to calculate plant height, its aim to research influence of vegetation cover on vegetation height. However, although these existing methods can be used to realize precision spray after obtaining plant basic information. But these methods must have the premise which the plants are placed in front of sensor. These sensor cannot identify plants by itself. Therefore, the sensor that can identify plants by itself should be used. It is natural to attempt to use vision identification plant and then perform precision spraying operation [24].

In this paper, the height characteristics of plant are mainly obtained by depth sensor. The sensor is used to identify plant and calculate plant height by using the depth camera and RGB color camera. The height of the plant can be calculated by both depth data and plant height in pixel. Once the height of plant and leaves distribution information are identified, the upper controller (Jetson TK1®) will send spray commands to control nozzles to open or close. These nozzles are fixed in vertical direction at different height. Furthermore, these nozzles are independent from each other. Different combinations of nozzles can be used depending on plant height. It aims to achieve the purpose of pesticide precision spraying.

The rest of the paper is organized as follows. In Section I, system working principle, sensor introduction and calibration, depth data acquisition, color and depth data processing are presented. In Section II, plant height measurement has been presented. In Section III, spray control system is presented. In Section IV, experimental validation with experiment setup and results are presented. Section V concludes this paper.

II. SYSTEM DESCRIPTION AND DATA PROCESSING

A. SYSTEM WORKING PRINCIPLE

There are variety forms of pesticide precious spraying, and there are a little differences in the different approaches [25]. But in any case, it can be explained by Fig. 1.

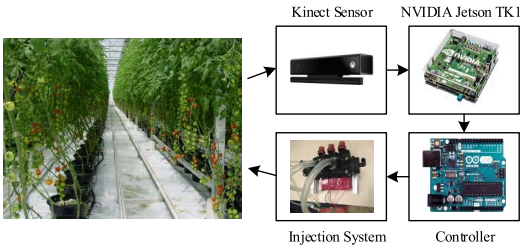

FIGURE 1. System operation principle.

Kinect sensor is used to collect visual information, it is the beginning of the whole process. Because this paper need the camera that has the function of distance measurement, so the sensor developed by Microsoft is chosen, and it has the characteristics of high resolution and high data transmission speed.

Tk1 platform module is used to process video frame data transmitted from sensor and send commands to controller. Tk1 has characteristics of high process speed, compact size and so on.

The controller used in this paper is arduino. Controller is mainly used to receive signal from TK1 platform, at the same time, open or close signal is transmitted to injection system by controller.

The injection system receives signal from the controller, and it controls corresponding nozzles open or close.

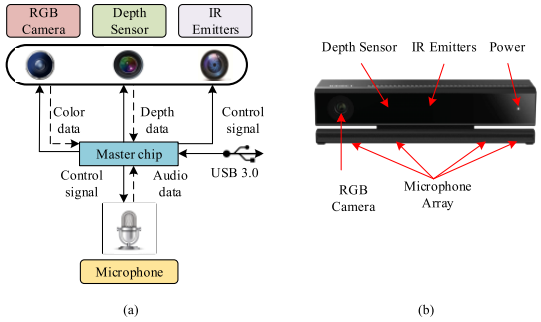

FIGURE 2. Schematic diagram and front view of Kinect.

B. SENSOR INTRODUCTION AND CALIBRATION

In this paper, Kinect as the sensor is used to identify plant height according to the depth data. In Fig. 2(a), it is the schematic diagram of sensor. The sensor is composed by a RGB camera, a depth sensor, an infrared radiation (IR) emitter and a multi-array microphone [26]. The sensor can send control signals to RGB camera, depth sensors, IR emitter and multi-array microphone. If these parts receive control signal, the RGB camera will return color image to master chip, depth sensor returns depth image to master chip, the microphone array returns master chip audio data correspondingly. The entire master chip system is connected to computer by USB 3.0 interface.

In Fig. 2(b), it is the front view of sensor. The infrared emitters and infrared cameras are combined to produce deep images. At the same time, the RGB camera will capture the corresponding color image.

Due to subsequent operation, the RGB image is processed firstly, and then obtain specific area where depth value is extracted. Secondly, depth value of corresponding area will be obtained in depth image [27].

Commonly, there is a certain distance between the depth sensor and the color camera, so this will cause a certain deviation between the depth image and RGB image [28], [29]. Therefore, sensor calibration work should be done first before using the sensor sensor accurately.

Sensor calibration is that establish constraints and solve the intrinsic parameters. Because the sensor has both depth sensor and RGB camera, so the relative position and pose parameters between depth sensor and RGB camera should be calibrated.

The calibration between the color sensor and the depth sensor can be performed by projection transformation. Actually, the pixels of the color image are the projection of the corresponding points in the three-dimensional space. Taking into account practical application and simplify the calculation, the rotation vector and translation vector are considered for the system only. Therefore, the coordinate transformation between depth sensor and RGB color camera can be expressed by following formula (1):

$$\begin{bmatrix} x \\ y \\ z \end{bmatrix} = R \times \begin{bmatrix} X \\ Y \\ Z \end{bmatrix} + T, \tag{1}$$

where vector R and T represent the rotation matrix and the translation matrix respectively. The (X,Y,Z) represents the coordinates of the corresponding points of the depth sensor. Similarly, the (x,y,z) represents coordinates of the corresponding points in the RGB color camera. The coordinates of the corresponding RGB color image can be expressed as follows (2):

$$\begin{bmatrix} u \\ v \end{bmatrix} = \begin{bmatrix} f_x \times \frac{x}{z} \\ f_y \times \frac{y}{z} \end{bmatrix} + \begin{bmatrix} c_x \\ c_y \end{bmatrix}, \tag{2}$$

where the parameter f_x and f_y represent the focal length of the camera in the x and y direction respectively. Whats more, both the parameter f_x and f_y are the internal parameters of the camera. The center of the chip and optical axis does not always overlap, so there are offsets in x and y direction, these offsets are represented with c_x and c_y in the x and y direction respectively.

C. DEPTH DATA ACQUISITION

Depth data obtained by depth sensor does not exactly correspond to the actual distance, but there is a certain deviation. If the depth data is expressed in pixel, when the distance between the object and camera changes, the difference between depth data and actual distance also changes, and this changing is non-linear. Curve line is obtained by comparison between actual distance and the sensor measured depth data. The curve line shows that when the distance is 1m, the sensor accuracy is 3mm; when the distance is 3m, Kinect accuracy is 30mm. In other words, the accuracy is gradually decreasing as distance increasing.

In order to avoid above situation, the depth data in pixels should be converted to data in real distance in millimeter. Assume depth data of raw value of the 3D scene point P is composed by 11 bit values. The real distance can be computed by following formula (3) developed by Juan R. Terven [30]:

$$d = Ktan(hd_{raw} + L) - O, \tag{3}$$

where variable d is the real distance between object and sensor in millimeter. Once the real distance is obtained by (3), the complete coordinate vector of point p can be derived [30], in other words, the actual position of point p can be obtained. Assume that the coordinate (i,j) is projection of point p. And the point p in 3D scene coordinate can be calculated in millimeter according the following formula (4), (5), (6):

$$x = (i - c_x) f_x d, \tag{4}$$

$$y = (j - c_y) f_y d, \tag{5}$$

$$z = d, \tag{6}$$

where $= 0.594214$, $f_y = 0.591045$, $c_x = 339.30$ and $c_y = 242.73$.

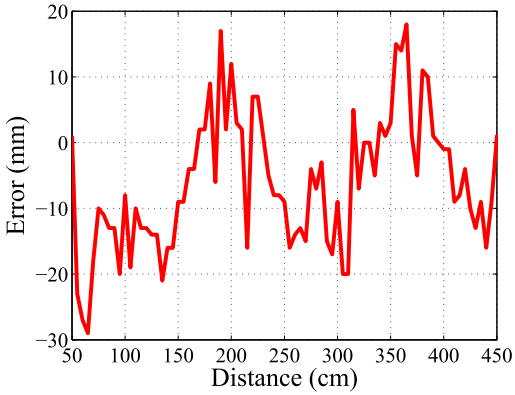

FIGURE 3. Depth data conversion.

The depth data is converted into the actual distance after using (3). And experiment is carried out to verify conversion result between depth data and actual distance. The result is shown in Fig. 3. The experimental results show that the error between the distance measured by manual work and sensor depth data is less than 30mm. There is change existing suddenly when distance is between 50cm and 60cm, this reason for the phenomenon is that it is dead zone in this range. And the result is within the allowable range of error.

D. COLOR AND DEPTH DATA PROCESSING

E. COLOR DATA PROCESSING

In order to identify plant height automatically by sensor installed on automatic guided vehicle and achieve the purpose of precision spraying pesticides, the green plant identification should be done firstly. The specific steps are shown in Fig. 4.

The RGB color data processing can be mainly divided several parts. In order to reduce the computation amount of the subsequent image processing, the image resolution of 1920*1080 is changed into 960*540. Secondly, the median filter is used to remove the salt-and pepper noise in this image. Erosion and dilation operation in mathematical morphological algorithm can remove small noise.

Actually, the RGB channel does not reflect the specific color information of the object well [31]. On the contrary, HSV color space can be intuitive expression of hue, saturation and lightness, and it is convenient to compare different color. Therefore, this paper uses the HSV space instead of RGB space to describe color character here. Thirdly, determine whether the HSV component of each pixel in the whole

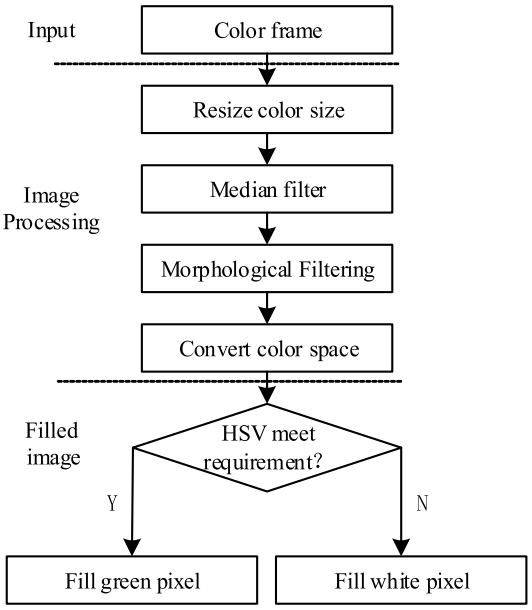

FIGURE 4. Color data processing.

image satisfies the green range requirement. Here, the paper assumes that green pixel component in HSV space meets the range [32], [33]: the hue is greater than 35 and less than 77, saturation is greater than 43 and less than 255, lightness is greater than 46 and less than 255. The following image are the processing results.

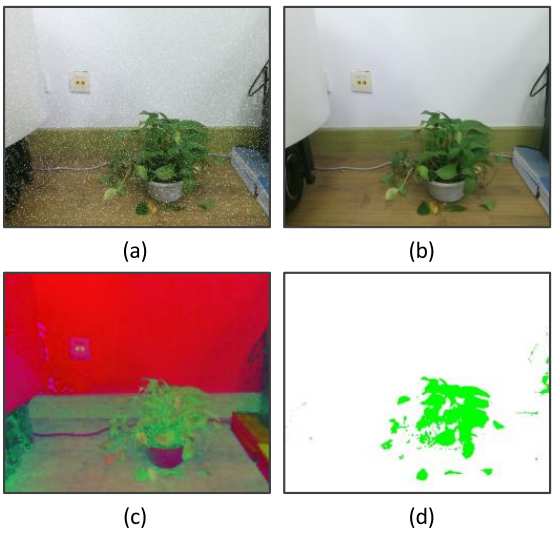

FIGURE 5. Fill green image.

Fig. 5(a) is the image contaminated by the salt-and pepper noise. For the salt-and-pepper noise, the median filter can filter out well. Fig. 5(b) is the result by applying median filter which its aperture linear size is set to 3. Fig. 5(b) shows that numerous noise is filtered out by median filter. When describing color character, the HSV color space is used instead of RGB color space, so the RGB color space is converted into HSV color space, and the conversion result is shown in Fig. 5(c). For the image of HSV space, it is easy to identify color of object. For those pixel that meets green range requirements are filled with green, and if the pixel that do not meets green range requirements is filled with white. Fig. 5(d) is the filling result according HSV space component requirements. Fig. 5(d) only contains green and white color. Therefore, the pixel height of green plant in HSV space image can be calculated easily.

F. DEPTH DATA PROCESSING

Before measuring the actual height of the green plant using the sensor, the actual distance between the plant and the sensor should be calculated firstly. Due to sensor field of vision, the depth data contain two parts, the first is the depth data of green plant, in addition, the depth data of other irrelevant object. But we only need the depth data of green plant. Therefore, irrelevant depth data should be filtered out. Contrast to the depth data, the green plants can be identified by the HSV data, so the green plants can be identified by the HSV color data. Once the position of the green plant in the pixel coordinate system of color image is determined, because the sensor has been calibrated at previous part, the position of green plant in pixel coordinate system of depth image is determined too. Finally, the real distance of green plant can be obtained by the depth sensor. The specific steps are shown in Fig. 6.

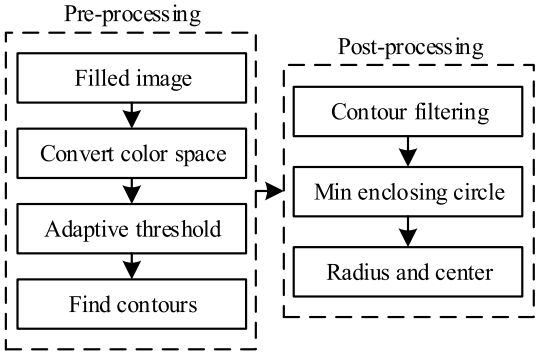

FIGURE 6. Finding green plant position.

The filled image consists white and green color only. In order to reduce the computation amount of the subsequent image processing, the color space is converted into gray space from RGB color space. Since the operation of finding contours can only be done on the base of binary image. So the image needs to be binarized with white and black. After the operation of finding contours, there are a lot of noise contours in the gray coordinate. These noise contours can be filtered out by length and area. Finally, the min enclosing circle that can surround the green plant can be obtained. At the same time, the radius and the center point can be gained. The following images shown in Fig. 7 are the processing results. Fig. 7(a) is the HSV image obtained by above steps. Fig. 7(b) represents the gray image from the color image, grayscale

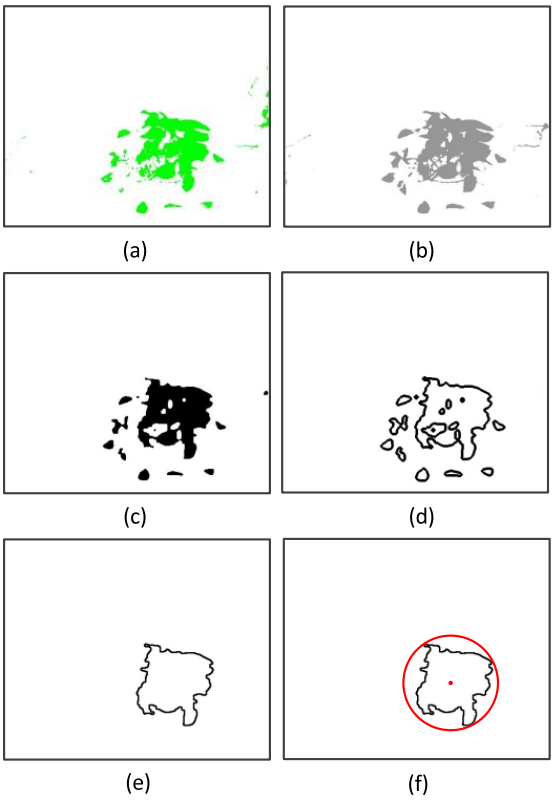

FIGURE 7. Finding radius and center point.

can reduce the amount of computation. Fig. 7(c) represents the adaptive threshold image by binary. And the binarized image is prepared for finding contours operations. Fig. 7(d) is obtained by finding contours operation. Fig. 7(d), there are existing noise contours, so these noise contours should be filtered out according to length and area of contours. Fig. 7(e) is obtained by filter operation of length and area. It filter out other noise contours and reserve green plants contours. Finally, the min enclosing circle that surrounds the green plant contour will obtained in Fig. 7(f). Furthermore, the center point and radius can be gained. Therefore, the next steps need to calculate average depth data in the range of min enclosing circle of depth image, thereby the real distance between the sensor and green plant can be calculated by Fig. 8.

In order to get the actual distance between the green plants and the sensor, the radius and the center point information of min enclosing circle is used [34]. In Fig. 8, firstly, the each pixel of depth image is traversed from pixel point $p(x,y)$, where x is equal to difference that x-axis of center point minus radius, and where y is equal to difference that y-axis of center point minus radius. Secondly, determine whether the traversed pixel is inside of min enclosing circle. If not, traverse the next pixel in order. On the contrary, determine whether the pixel is green point. If not, traverse the next pixel in order. On the contrary, calculate the depth data. Because a lot of pixels meet the requirement above in the min

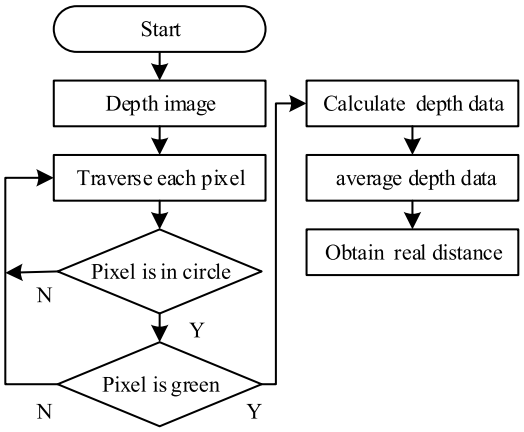

FIGURE 8. Depth data processing.

enclosing circle. Therefore, in order to obtain the actual distance between the plant and the sensor, it is necessary to find the average value of the depth data of the pixel satisfying the requirements. Finally, the actual distance between the depth sensor and the plant can be computed.

III. PLANT HEIGHT MEASUREMENT

The actual distance between the sensor and green plant has been obtained by previous steps [35], the actual green plant height can be obtained by corresponding proportional relationship [36], [37]. The specific diagram is shown in Fig. 9.

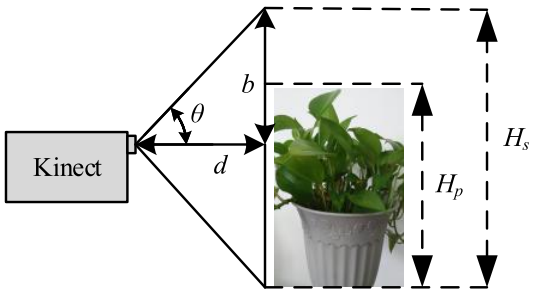

FIGURE 9. Plant height measurement.

Usually, each camera has a field of view, the focal length will determine the viewing angle. The horizontal and vertical field of view of the sensor are 70° and 60° respectively [26], [38]. If the real distance between the plant and the sensor camera is calculated, the height of the plant can be calculated according to the following formulas [39], it is shown as following (7), (8), (9):

$$b = d \times tan\theta, \tag{7}$$

$$\frac{H_p}{H_s} = \frac{H_r}{2b}, \tag{8}$$

$$H_r = \frac{H_p}{H_s} \times 2b, \tag{9}$$

where the variable b is the half height of background, and where the variable d is the actual distance between the sensor

and green plant, the variable θ is half of vertical field view of the sensor. The variable H_p is the plant height in pixel. The variable H_r is actual height of plant to be detected in 3D space. The variable H_s is height of background in pixel and H_s is equal to 424 in pixel and Variable θ is equal to 30° [38].

Since the maximum depth range of Kinect for xbox one is 4500mm and the minimum depth range is 500mm. According to the above formula, the highest plant height that can be measured is 577mm when actual distance is 500mm, and the highest plant height that can be measured is 5196mm when actual distance is 4500mm.

IV. SPRAY CONTROL SYSTEM

The pesticide spray control is the most important part in whole system. Its driving signal is mainly from the arduino controller. Different control signals will cause different combinations of solenoid valves. On the side of the automatic guided vehicle, there are three nozzles that are installed in vertical column direction. AGV total height is 750mm, there is a nozzle installed every 150mm. It is shown in Fig. 10. Each nozzle can spray with the highest height of 300mm, and the extreme spraying height of whole system is 900mm with three nozzles opening.

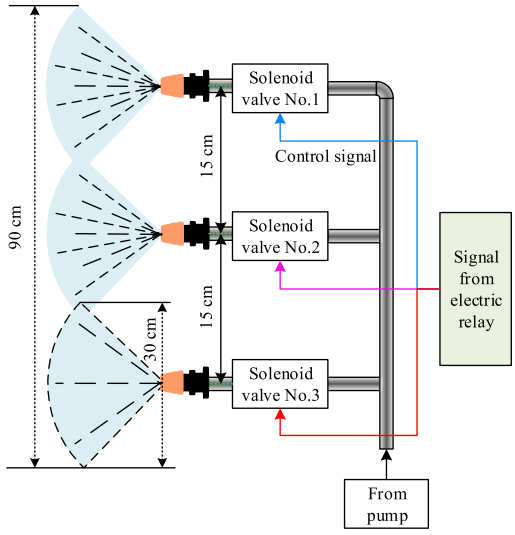

FIGURE 10. Nozzle installation diagram.

In order to achieve precise pesticide spraying for plants, it is necessary to open different combinations of solenoid valve according to different plant height, and thereby system can control spray height. Therefore, the rules of combination of solenoid valve open or close can be explained by Table 1:

Due to the limited height of automatic guided vehicle, the highest plant that the system can be sprayed is about 900mm. The solenoid valve combination methods can be divided into five cases. Case 1, when the system do not identify plant, it need to closed all solenoid valve; case 2, when the height of plant identified is less than 300mm, No.3 solenoid valve is open only; case 3, when the height of plant identified is greater than 300mm and less than 600mm, No.3 and No.2 solenoid valve are opened only; case 4, when the height of plant identified is greater than 600mm and less than 900mm, all solenoid valves are opened; case 5, if the plant height is greater than 900mm, due to the limitations of the system itself, although some of top plant leaves cannot be sprayed, but all the solenoid valves are opened.

TABLE 1. Nozzle combination methods.

Case	Height (cm)	Combination method
1	None	Close all
2	height <30	Only open No.3
3	30 <Height <60	Open No.3 and No.2
4	60 <Height <90	Open all
5	90 <Height	Open all

V. EXPERIMENTAL VALIDATION

In order to verify above proposed method based on height of plant to automatically open or close corresponding valve installed on automatic guided vehicle, large number of experiments have been carried out. The pesticide spraying system of height-adaptive test bench is introduced as following.

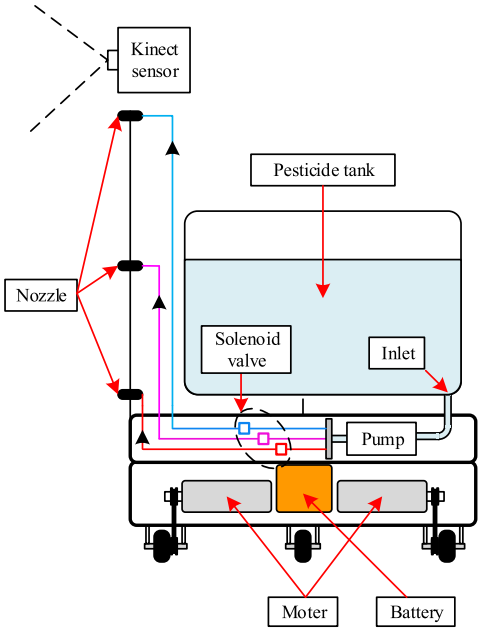

FIGURE 11. Schematic diagram and front view of system.

In Fig. 11, it is the front view schematic diagram of all pesticide system. The main part include a DC motor that provides power for the system, the sensor that provides vision information for the system, three solenoid valves that receive commands sent by arduino controller and send commands to control nozzles open or close, a pesticide tank that store pesticide, a pump that sucks pesticide from pesticide tank and pump it to different nozzles according to requirement.

A. EXPERIMENTAL SETUP

In order to be able to effectively verify proposed system, the system is placed to three different plant heights. It aims to measure plant height by sensor and identify state of nozzles.

In front of system about 1000mm, it is followed by placing three plants with different height from each other. Its height are 230mm, 510mm and 810mm, respectively. The system moves forward evenly and detects plant height simultaneously. In process of moving forward, the number of height detection for each plant can reach 80 times. The system can confirm the plant height by these 80 results.

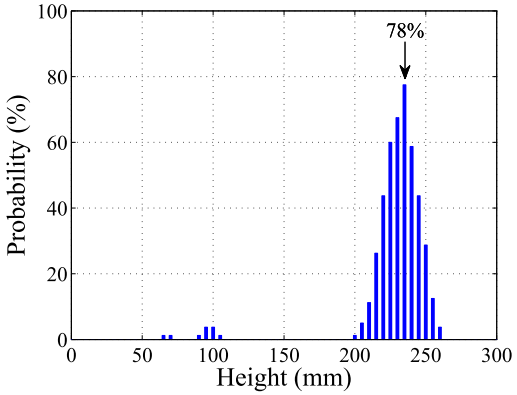

FIGURE 12. Height statistics for first plant.

B. EXPERIMENTAL RESULTS

In Fig. 12, Fig. 14 and Fig. 16, the x-axis represents height of plant. However, in Fig. 12, the y-axis represents that size of probability that 80 measurement results are in the interval of (0-5), (5-10). . .(295-300), in Fig. 14, the y-axis represents that size of probability that 80 measurement results are in the interval of (0-5), (5-10). . .(825-830), in Fig. 16, the y-axis represents that size of probability that 80 measurement results are in the interval of (0-5), (5-10). . .(995-1000).

When system measures plant height, there is large deviation because of system and sensor errors, so plant height measurement final result can be obtained by selecting height with maximum probability. In Fig. 12, the maximum probability is 78%, and it is corresponding to height of 235mm. In Fig. 14, the maximum probability is 68%, and it is corresponding to height of 540mm. In Fig. 16, the maximum probability is 68%, and it is corresponding to height of 780mm. And these height values are shown In Fig. 13, Fig. 15 and Fig. 17 respectively and represented by using black line.

In Fig. 13, Fig. 15 and Fig. 17 the black line indicates the actual plant height measured by sensor. In order to illustrate the accuracy of algorithm, the upper and lower limits of error value are set. The error value is equal to 5% of black line value. For different height plants, the error value is different and upper and lower limits are presented with blue line. The area between two blue lines is said the credible interval. The upper limit of three plants are 246.75mm, 567mm and 819mm respectively, and the lower limit of three plants are 223.25mm, 513mm and 741mm.

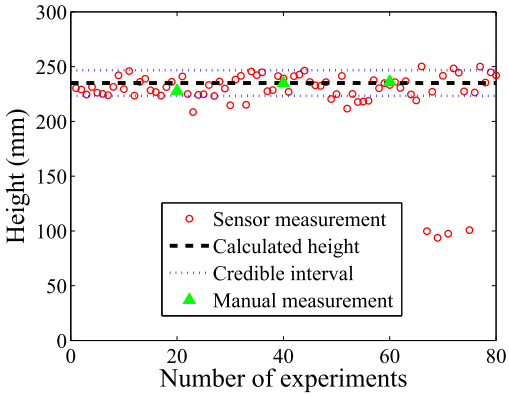

FIGURE 13. Height calculation for first plant.

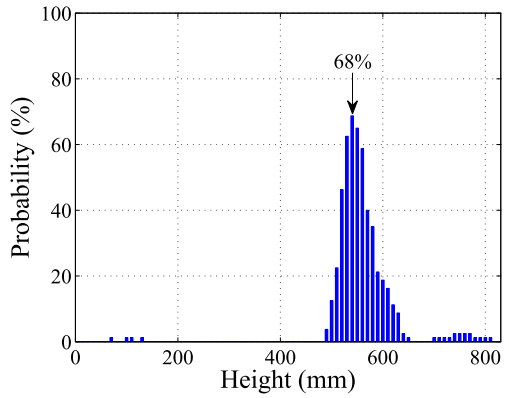

FIGURE 14. Height statistics for second plant.

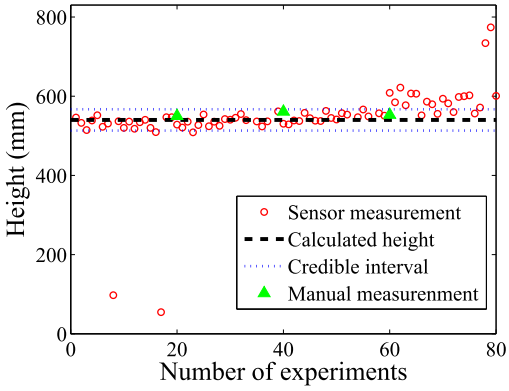

FIGURE 15. Height calculation for second plant.

When plant height is within this interval, it is believed the plant height measurement error is acceptable by sensor. The red circles represent the results of plant height measurement by sensor.

In order to demonstrate accuracy of sensor measurement results, each plant is measured three times by manual work and it is represented by green filled triangles. The height of first plant measured by manual work is 228mm, 235mm and 236mm. The height of second plant measured by manual work is 550mm, 561mm and 553mm. The height of third plant measured by manual work is 755mm, 760mm and 771mm. The results show that these green filled triangles

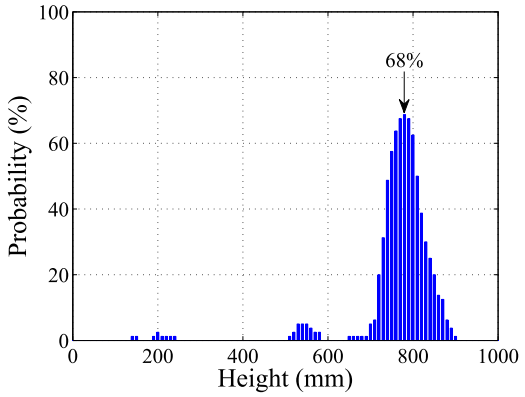

FIGURE 16. Height statistics for third plant.

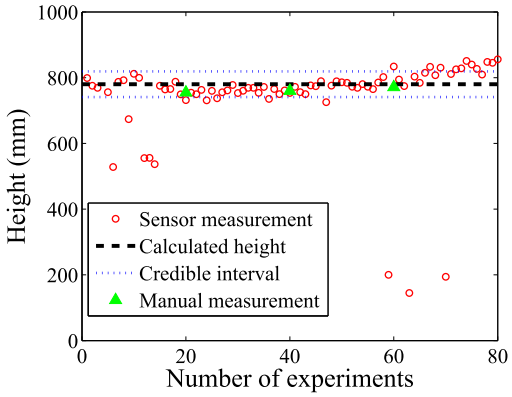

FIGURE 17. Height calculation for third plant.

are all within credible interval, which proves the accuracy using sensor to measure plant height.

The sensor is used to measure three different height plant in above section, and the accuracy of height measurement has been demonstrated. The system should open different number of nozzles according to rules set in Table.1. In order to able to calculate number of nozzles which its state is open or close more directly, the flow meter is used to collect total outlet flow information. If the number of open is different, the total outlet flow of system is also different.

In above section, the height measured by sensor are 235mm, 540mm and 780mm. So the nozzle number of open should be 1, 2 and 3 respectively. The flow rate result is shown as Fig. 18.

The x-axis represents time (ms) and the y-axis represents flow rate (L/min) of pump. The pump is pressure-controlled. The pump is opened when pump pressure is less than 0.1Mpa and the pump is closed when pump pressure is over than 0.45Mpa. The self-suction height of water pump is 2m.

As shown in Fig. 18, when there is no plants, the total flow rate is 0L/min. When height of plant is 235mm measured by sensor, the system will only open one nozzle and the flow rate is between 1.3L/min and 1.5L/min. When height of plant is 540mm measured by sensor, the system will open two nozzles and flow rate is controlled near 2.3L/min. When height of plant is 780mm measured by sensor, the system will

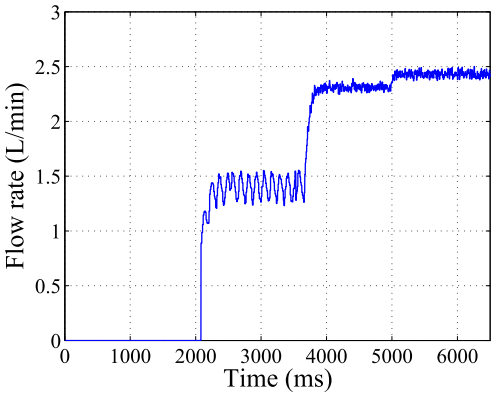

FIGURE 18. Number of nozzles for spraying.

open three nozzles and flow rate is controlled near 2.4L/min. So when the system moves forward evenly, No.1, No.2 and No.3 nozzle are opened automatically according to the plant height.

Since the nozzles used in this system are larger in diameter, the flow rate generated by two nozzles is substantially equal to the rated flow of the pump. Thus, as shown in Fig. 18, when the first nozzle is opened, flow rate generated is about half of the rated flow of pump, the flow rate is about 1.4L/min. When two nozzles are opened, the flow rate is close to the rated flow of pump, the flow rate is about 2.3L/min. And flow rate is 0.9L/min lager than only one nozzle opened. When three nozzles are opened, total flow of the system has reached the rated flow, the flow rate is 2.4L/min. Compared to open the two valves, the total flow rate is only 0.1L/min larger than two nozzles opened.

VI. CONCLUSION

In this paper, a height-adaptive pesticide spraying system is proposed. The system is based on automatic guided vehicle. Using depth data to obtain real distance between the plant and camera. The height of plant can be calculated by combining with vertical field of the sensor. And control the solenoid valve open or close by controller. The system can identify plant height accurately, and system can open or close corresponding nozzles according to height information, this illustrates effectiveness of the proposed design method. In the future research, we will focus on the more advanced method suitable for height-adaptive pesticide spraying system.

REFERENCES

[1] P. Sabatier *et al.*, "Long-term relationships among pesticide applications, mobility, and soil erosion in a vineyard watershed," *Proc. Nat. Acad. Sci. USA*, vol. 111, no. 44, pp. 15647–15652, 2014.

[2] S. Stehle and R. Schulz, "Agricultural insecticides threaten surface waters at the global scale," *Proc. Nat. Acad. Sci. USA*, vol. 112, no. 18, pp. 5750–5755, 2015.

[3] G. Doruchowski and R. Holownicki, "Environmentally friendly spray techniques for tree crops," *Crop Protection*, vol. 19, nos. 8–10, pp. 617–622, 2000.

[4] R. Oberti *et al.*, "Selective spraying of grapevines for disease control using a modular agricultural robot," *Biosyst. Eng.*, vol. 146, pp. 203–215, Jun. 2016.

[5] H. R. Karimi and H. Gao, "New delay-dependent exponential H_∞ synchronization for uncertain neural networks with mixed time delays," *IEEE Trans. Syst., Man, Cybern. B, Cybern.*, vol. 40, no. 1, pp. 173–185, Feb. 2010.
[6] J. S. West, C. Bravo, R. Oberti, D. Lemaire, D. Moshou, and H. A. Mccartney, "The potential of optical canopy measurement for targeted control of field crop diseases," *Annu. Rev. Phytopathol.*, vol. 41, no. 41, pp. 593–614, 2003.
[7] M. Malneršič, M. Dular, B. Širok, R. Oberti, and M. Hočevar, "Close-range air-assisted precision spot-spraying for robotic applications: Aerodynamics and spray coverage analysis," *Biosyst. Eng.*, vol. 146, pp. 216–226, Jun. 2016.
[8] Q. Lu, L. Zhang, P. Shi, and H. R. Karimi, "Control design for a hypersonic aircraft using a switched linear parameter-varying system approach," *Proc. Inst. Mech. Engin. I, J. Syst. Control Eng.*, vol. 227, no. 1, pp. 85–95, 2013.
[9] R. Bogue, "Robots poised to revolutionise agriculture," *Ind. Robot, Int. J.*, vol. 43, no. 5, pp. 450–456, 2016.
[10] A. Bechar and Y. Edan, "Human-robot collaboration for improved target recognition of agricultural robots," *Ind. Robot, Int. J.*, vol. 30, no. 5, pp. 432–436, 2003.
[11] K. Sabanci and C. Aydin *et al.*, "Image processing based intelligent spraying robot for weed control," *Fresenius Environ. Bull.*, vol. 25, no. 12, p. 5305, 2016.
[12] E. Gil, A. Escola, J. R. Rosell, S. Planas, and L. Val, "Variable rate application of plant protection products in vineyard using ultrasonic sensors," *Crop Protection*, vol. 26, no. 8, pp. 1287–1297, 2007.
[13] J. Backman, T. Oksanen, and A. Visala, "Navigation system for agricultural machines: Nonlinear model predictive path tracking," *Comput. Electron. Agricult.*, vol. 82, no. 1, pp. 32–43, 2012.
[14] D. K. Giles and D. C. Slaughter, "Precision band spraying with machine-vision guidance and adjustable yaw nozzles," *Trans. ASAE*, vol. 40, no. 1, pp. 29–36, 1997.
[15] H. Maghsoudi, S. Minaei, B. Ghobadian, and H. Masoudi, "Ultrasonic sensing of pistachio canopy for low-volume precision spraying," *Comput. Electron. Agricult.*, vol. 112, pp. 149–160, Mar. 2015.
[16] F. Solanelles, S. Planas, J. R. Rosell, F. Camp, and F. Gràcia, "An electronic control system for pesticide application proportional to the canopy width of tree crops," *Biosyst. Eng.*, vol. 95, no. 4, pp. 473–481, 2006.
[17] D. L. Brown, D. K. Giles, M. N. Oliver, and P. Klassen, "Targeted spray technology to reduce pesticide in runoff from dormant orchards," *Crop Protection*, vol. 27, nos. 3–5, pp. 545–552, 2008.
[18] E. Moltó, B. Martin, and A. Gutiérrez, "PM—Power and machinery: Pesticide loss reduction by automatic adaptation of spraying on globular trees," *J. Agricult. Eng. Res.*, vol. 78, no. 1, pp. 35–41, 2001.
[19] S. D. Tumbo, M. Salyani, J. D. Whitney, T. A. Wheaton, and W. M. Miller, "Investigation of laser and ultrasonic ranging sensors for measurements of citrus canopy volume," *Appl. Eng. Agricult.*, vol. 18, no. 3, pp. 367–372, 2002.
[20] T.-T. Lin, C.-F. Chien, W.-C. Liao, K.-C. Chung, and J.-M. Chang, "Machine vision systems for plant growth measurement and modeling," *Environ. Control Biol.*, vol. 44, no. 3, pp. 181–187, 2010.
[21] R. Sui and J. A. Thomasson, "Ground-based sensing system for cotton nitrogen status determination," *Trans. ASABE*, vol. 49, no. 6, pp. 1983–1991, 2006.
[22] T. Fricke and M. Wachendorf, "Combining ultrasonic sward height and spectral signatures to assess the biomass of legume–grass swards," *Comput. Electron. Agricult.*, vol. 99, no. 7, pp. 236–247, 2013.
[23] S. Luo *et al.*, "Estimation of wetland vegetation height and leaf area index using airborne laser scanning data," *Ecol. Indicators*, vol. 48, pp. 550–559, Jan. 2015.
[24] M. Gonzalez-de-Soto, L. Emmi, M. Perez-Ruiz, J. Aguera, and P. Gonzalez-de-Santos, "Autonomous systems for precise spraying—Evaluation of a robotised patch sprayer," *Biosyst. Eng.*, vol. 146, pp. 165–182, Jun. 2016.
[25] D. C. Slaughter, D. K. Giles, and D. Downey, "Autonomous robotic weed control systems: A review," *Comput. Electron. Agricult.*, vol. 61, no. 1, pp. 63–78, 2008.
[26] A. Corti, S. Giancola, G. Mainetti, and R. Sala, "A metrological characterization of the Kinect V2 time-of-flight camera," *Robot. Auto. Syst.*, vol. 75, pp. 584–594, Jan. 2016.
[27] D.-M. Córdova-Esparza, J. R. Terven, H. Jiménez-Hernández, and A.-M. Herrera-Navarro, "A multiple camera calibration and point cloud fusion tool for Kinect V2," *Sci. Comput. Program.*, vol. 143, pp. 1–8, Sep. 2017.
[28] K. Khoshelham, "Accuracy analysis of Kinect depth data," *Int. Arch. Photogram., Remote Sens. Spatial Inf. Sci.*, vol. 38, no. 5, pp. 133–138, 2012.
[29] G. Marin, F. Dominio, and P. Zanuttigh, "Hand gesture recognition with jointly calibrated leap motion and depth sensor," *Multimedia Tools Appl.*, vol. 75, no. 22, pp. 14991–15015, 2016.
[30] V. Frati and D. Prattichizzo, "Using Kinect for hand tracking and rendering in wearable haptics," in *Proc. World Haptics Conf.*, 2011, pp. 317–321.
[31] V. Chernov, J. Alander, and V. Bochko, "Integer-based accurate conversion between RGB and HSV color spaces," *Comput. Electr. Eng.*, vol. 46, pp. 328–337, Aug. 2015.
[32] S. Romani, P. Sobrevilla, and E. Montseny, "Variability estimation of hue and saturation components in the HSV space," *Color Res. Appl.*, vol. 37, no. 4, pp. 261–271, 2012.
[33] M. Guijarro, G. Pajares, I. Riomoros, P. J. Herrera, X. P. Burgos-Artizzu, and A. Ribeiro, "Automatic segmentation of relevant textures in agricultural images," *Comput. Electron. Agricult.*, vol. 75, no. 1, pp. 75–83, 2011.
[34] J. X. Du, C. M. Zhai, and Q. P. Wang, "Recognition of plant leaf image based on fractal dimension features," *Neurocomputing*, vol. 116, pp. 150–156, Sep. 2013.
[35] Z. Wang, X. Song, S. Wang, J. Xiao, R. Zhong, and R. Hu, "Filling Kinect depth holes via position-guided matrix completion," *Neurocomputing*, vol. 215, pp. 48–52, Nov. 2016.
[36] D. Reiser, J. M. Martín-López, E. Memic, M. Vázquez-Arellano, S. Brandner, and H. W. Griepentrog, "3D imaging with a sonar sensor and an automated 3-axes frame for selective spraying in controlled conditions," *J. Imag.*, vol. 3, no. 1, p. 9, 2017.
[37] Y. Jiang, C. Li, and A. H. Paterson, "High throughput phenotyping of cotton plant height using depth images under field conditions," *Comput. Electron. Agricult.*, vol. 130, pp. 57–68, Nov. 2016.
[38] H. Gonzalez-Jorge *et al.*, "Metrological comparison between Kinect I and Kinect II sensors," *Measurement*, vol. 70, pp. 21–26, Jun. 2015.
[39] A. Traumann, M. Daneshmand, S. Escalera, and G. Anbarjafari, "Accurate 3D measurement using optical depth information," *Electron. Lett.*, vol. 51, no. 18, pp. 1420–1422, 2015.

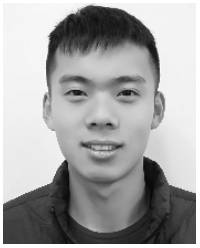

TINGKAI CHEN received the B.Sc. degree in marine engineering from Shanghai Maritime University, Shanghai, China, in 2016, where he is currently pursuing the M.Sc. degree in marine engineering. His research interests include machine vision, target tracking, feature analysis, and image processing.

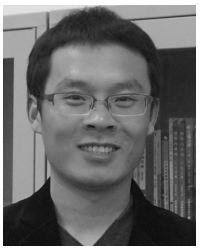

FEI MENG (M'16) received the Ph.D. degree in mechanical engineering from the Beijing Institute of Technology, Beijing, China, in 2014. He is currently an Associate Professor with the Merchant Marine College, Shanghai Maritime University, China. His research interests include control of dynamical systems, optimal control, and networked control system. In the past five years, he has contributed over 20 papers in refereed journals and conference proceedings. He serves as a Reviewer for many journals, including the IEEE/ASME TRANSACTIONS ON MECHATROICS, the IEEE TRANSACTIONS ON VEHICULAR TECHNOLOGY, the *Mechanical Systems and Signal Processing*, the *Journal of the Franklin Institute*, and the *International Journal of Vehicle Design*.